*Meteoritics & Planetary Science* 36, 1027–1038 (2001)
Available online at http://www.uark.edu/meteor

# Korra Korrabes: A new, large H3 chondrite breccia from Namibia

L. D. ASHWAL

Department of Geology, Rand Afrikaans University, P. O. Box 524, Auckland Park, 2006, South Africa
Author's e-mail address: LDA@na.rau.ac.za

*(Received 2000 December 20; accepted in revised form 2001 April 26)*

**Abstract**–A new, large, ordinary chondrite has been recovered from near the strewn field of Gibeon iron meteorites in Namibia, and is designated Korra Korrabes, after the farm property on which the specimens were found in 1996–2000. A total of ~140 kg of related specimens were recovered, including a large stone of 22 kg, and hundreds of smaller objects between 2 g and several kilograms. Cut surfaces indicate that Korra Korrabes is a breccia, containing 10–20% of light grey-brown clasts up to 3 cm across in a uniform, darker grey-brown host that contains abundant round chondrules, and irregular grains of Fe-Ni metal and troilite up to 1 cm across. The vast majority of the stone is unshocked, although some clasts show mild shock features (stage S2), and one chondrule fragment is moderately shocked (stage S3). Weathering grade varies between W1 and W2. Microprobe analyses indicate variable compositions of olivine ($Fa_{13.8-27.2}$, $n = 152$, percent mean deviation = 7.82%) and low-Ca pyroxene (multiply twinned clinobronzite, $Fs_{8.4-27.8}$, $n = 68$). There is excellent preservation of magmatic textures and mineralogy within many chondrules, including normally zoned olivine ($Fa_{13.8-18.9}$) and low-Ca pyroxene ($Fs_{0.2-20.9}$) phenocrysts, and abundant glass, some of whose compositions are unusually alkaline ($Na_2O + K_2O$ = 13.6–16.3 wt%) and Ca-deficient (CaO = 0–0.75 wt%), seemingly out of magmatic equilibrium with associated clinoenstatite or high-Al calcic clinopyroxene crystals. Textural and mineralogical features indicate that Korra Korrabes is an H3 chondrite breccia, which represents the largest and least equilibrated stony meteorite yet recovered from Namibia; it is now one of the four largest unequilibrated ordinary chondrites worldwide.

## INTRODUCTION

Namibian meteorites are well known, in part because of the occurrence at Hoba (Fig. 1) of an *in situ* ~60 ton IVB iron meteorite, which has been described as the world's largest (Spencer and Hey, 1932), and also because of the Gibeon IVA iron meteorite (Buchwald, 1969b), specimens of which continue to be widely distributed by mineral dealers and collectors. Since the 1973 publication by Frick and Hammerbeck of the *Catalogue of South African and South West African Meteorites*, the inventory of officially recognized, individual meteorites from Namibia (formerly South West Africa) has more than doubled to a present total of 19 (Table 1), including the new specimen described herein. During a routine search in 1996 for additional specimens of Gibeon, which are known to be distributed over an elliptical strewn field ~400 × 100 km across (Fig. 1), several pieces were taken of a large stone that was later confirmed as a new chondritic meteorite. In this paper, I describe and classify this new meteorite, which now represents the largest chondrite yet recovered in Namibia, and the world's fourth largest unequilibrated ordinary chondrite.

## HISTORY OF SAMPLE RECOVERY

The recent increased interest in meteorites as collectible items, with their concomitant rise in value, has led to fervent searches for specimens, especially by local residents in the area around Gibeon (Fig. 1), in which an abundance of iron meteorites have been recovered for many years. During such an effort in 1996 November, a local resident came upon a group of dark stones that he recognized as unusual; these stones were exposed at surface over a small area of about 20 $m^2$. Although obviously not iron meteorites, their overall dark colour and high apparent density suggested that these objects might represent something of value, and in 1998, 12 pieces, including a single large sample of ~22 kg were taken to Windhoek, where they were later discarded as novelties, and used as garden stones. The large stone was cemented, along with numerous other curious rock specimens, into a low garden wall. In 2000 August, one of the smaller pieces was acquired by Dr. R. McKenzie, and taken to Johannesburg, where L. D. A. confirmed its identity as a chondritic meteorite. Soon thereafter, most of the remaining material, including the large stone (which was carefully extracted from its place in the garden wall) was purchased by



Prelude preprint MS#4485

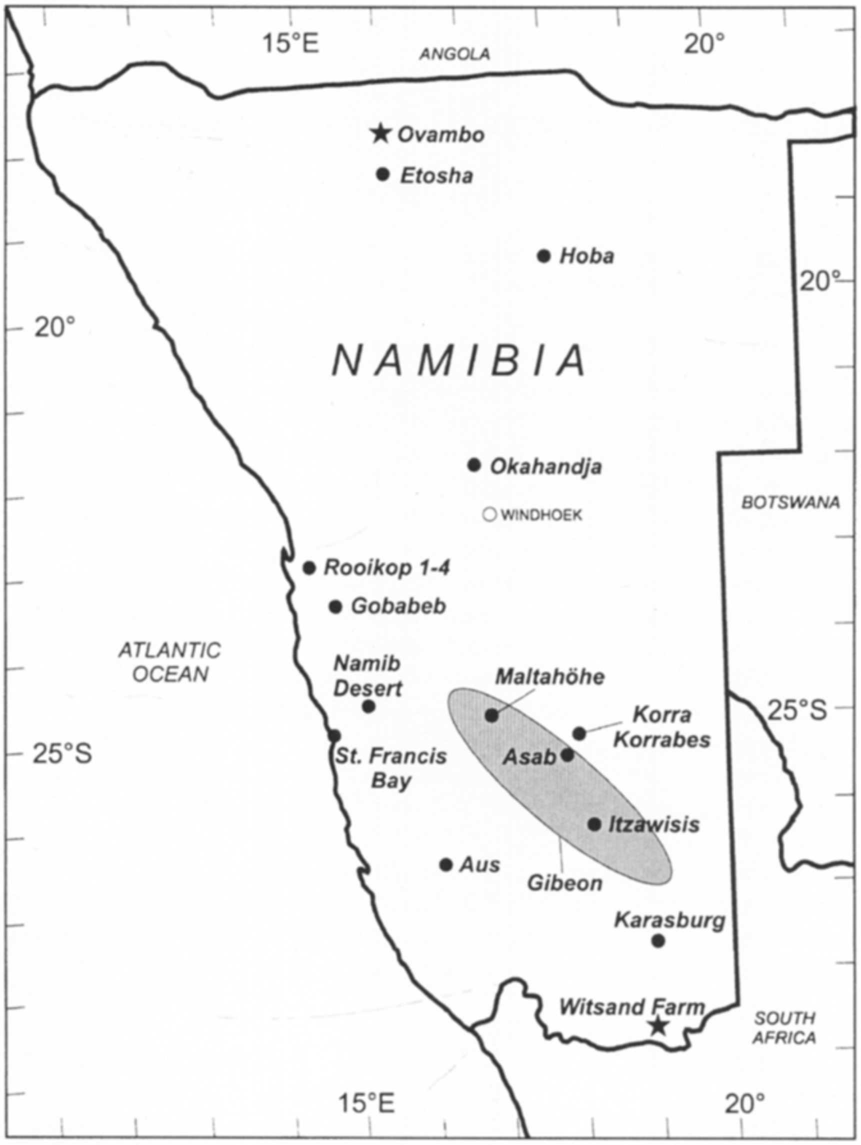


FIG. 1. Locations of meteorite falls (filled stars) and finds (filled circles) in Namibia, compiled from references given in Table 1. Specimens of the Gibeon IVA iron meteorite are distributed over a large strewn field, approximated by the shaded ellipse, with axes of ~400 km and ~100 km (Buchwald, 1969b). The Korra Korrabes H3 chondrite was recovered from northeast of the Gibeon strewn field.

Dr. McKenzie, and taken to Pretoria. In addition to the large specimen of 22 kg, 11 smaller stones with a collective mass of ~18 kg were recovered. During subsequent field investigations, several hundred additional pieces ranging from 2 g to several kilograms were collected. The total mass of recovered specimens is ~140 kg.

The recovery site is a dry riverbed about 35 km east-southeast of the town of Gibeon, and ~15 km southwest of Highway 1066. The coordinates of the site, as determined by GPS, are 25°12' S, 18°05' E; the location is near the southeast corner of the farm property Korra Korrabes 72 (Fig. 1). Following the guidelines set forth by the Meteoritical Society, the name Korra Korrabes is assigned to the meteorite, as the finding site is within this farm property; this proposal has been accepted by the Committee on Meteorite Nomenclature. Type specimens, which include a cut piece of 114.6 g and three small uncut pieces 22.3–30.1 g (total mass = 192.6 g) have been deposited in the Geosciences Museum, Pretoria, South Africa. Most of the remaining Korra Korrabes material, including the ~22 kg specimen, will be retained in the private collection of Dr. R. McKenzie. With a total mass of ~140 kg, Korra Korrabes is the largest stony meteorite yet recovered from Namibia (Table 1). The ~27 kg Gobabeb H4 chondrite, recovered in 1969 over 400 km northwest of Korra Korrabes (Fig. 1), is of similar type, although the present location of the main mass is uncertain (Fudali and Noonan, 1975). Interestingly, four small pieces (total mass = 1.53 kg) of an H5 chondrite were recovered in 1999 August at a site 38 km southwest of the Korra Korrabes

TABLE 1. Recognized meteorites from Namibia.

| Name | Classification | Location | Recovery details | Mass | Location of main mass (MM) or type specimen (TS) | References |
|---|---|---|---|---|---|---|
| Asab | H5 chondrite | 25°26' S; 17°55' E | Find: 1999 Aug. | 1.53 kg | MM: SW Meteorite Lab., Payson, Arizona (USA); TS: t.b.d. | Grossman (2001) |
| Aus | L chondrite | 26°40' S; 16°15' E | unknown | 30 g | MM: unknown; TS: Max Planck Inst., Heidelberg | – |
| Etosha | IC iron | ~18°30' S; ~16° E | unknown | 110.7 kg | MM: University Potchefstroom, South Africa | Scott and Wasson (1976) |
| Gibeon | IVA iron | ~25°10' S; ~18° E | Find: before 1836 | >15 tons? | MM: South African Museum, Cape Town | Buchwald (1969b, 1975) |
| Gobabeb | H4 chondrite | 23°33' S; 15°02' E | Find: 1969 | ~27 kg | MM: Windhoek State Museum, Namibia; 25 g fragments—Smithsonian, Washington, D. C. | Fudali and Noonan (1975) |
| Hoba | IVB iron | 19°35' S; 17°55' E | Find: 1920 | ~60 tons | MM: *in situ* | Spencer and Hey (1932); Buchwald (1975) |
| Itzawisis | Pallasite | 26°16' S; 18°11' E | Find: 1946 | 350 g | TS: (69 g): Transvaal Museum, Pretoria, South Africa | Frick & Hammerbeck (1973) |
| Karasburg | IIIAB iron | 27°40' S; 18°58° E | unknown | ~11 kg | stolen from MuseumAfrica, Johannesburg, 2000 Oct. | Buchwald (1969a) |
| Korra Korrabes | H3 chondrite breccia | 25°12' S; 18°05' E | Find: 1996 Nov. | ~140 kg | TS: Transvaal Museum, Pretoria, South Africa; MM: private collection, R. McKenzie, Pretoria | This study |
| Maltahöhe | IIICD iron | 24°55' S; 16°59' E | Find: 1991 | 22.3 kg | MM: private collection, M.D. Cilz, Malta, MT (USA) | Wlotzka (1991) |
| Namib Desert | H4 chondrite | 24°45' S; 15°22' E | Find: 1979 April 22 | ~1 kg | MM: Windhoek State Museum, Namibia | Graham (1981) |
| Okahandja | IIAB iron | 21°59' S; 16°56' E | known before 1926 | 6.6 kg | MM: Transvaal Museum, Pretoria, South Africa | Frick & Hammerbeck (1973) |
| Ovambo | L6 chondrite | ~18° S; ~16° E | Fall: ~1900 | 56 g | Finland? | Clarke (1975) |
| Rooikop 001 | H5 chondrite | 23°05' S; 14°42.9' E | Find: 1991 June | 1.039 kg | MM: Geology Survey of Nambia, Windhoek | Reid *et al.* (1995) |
| Rooikop 002 | L5 chondrite | 23°05' S; 14°42.9' E | Find: 1991 June | 0.903 kg | MM: Geology Survey of Nambia, Windhoek | Reid *et al.* (1995) |
| Rooikop 003 | L4/5 chondrite | 23°05' S; 14°42.9' E | Find: 1991 June | 0.902 kg | MM: Geology Survey of Nambia, Windhoek | Reid *et al.* (1995) |
| Rooikop 004 | L6 chondrite | 23°05' S; 14°42.9' E | Find: 1999 July | 1.248 kg | MM: Geology Survey of Nambia, Windhoek | Russell *et al.* (1999) |
| St. Francis Bay | L6 chondrite | 25°04' S; 14°53' E | Find: 1976 June 6 | 531.6 g | MM: Windhoek State Museum, Namibia | Graham (1978) |
| Witsand Farm | LL4 chondrite | 28°40' S; 18°55' E | Fall: 1880 Dec. 9 | 79.5 g | MM: Natural History Museum, London | Frick & Hammerbeck (1973) |

t.b.d. = to be determined.

locality (Fig. 1; Table 1); this meteorite has been designated Asab, after a nearby town (J. N. Grossman, pers. comm., 2000).

The Korra Korrabes chondrite is amongst the largest of known unequilibrated ordinary chondritic (UOC) meteorites worldwide. Other large specimens include Clovis (283 kg, find, New Mexico, USA, H3.6), Dimmitt (200 kg, find, Texas, USA, H3.7), Tulia (a) (86 kg, find, Texas, USA, H3-4), Zag (175 kg, fall, Western Sahara, H3-6) and Parnallee (78 kg, fall, Tamil Nadu, India, LL3.6). Korra Korrabes (~140 kg) can be considered the world's fourth largest UOC meteorite, regardless of whether the Dimmitt and Tulia specimens are paired (Huss, 1982).

## RESULTS

### Macroscopic Description

The Korra Korrabes specimens are dark, compact stones that readily attract a hand magnet. Their irregular surfaces are variably coated with a thin (generally <1 mm) layer of iron oxides and hydroxides (Fig. 2). Some pieces contain irregular fractures several centimeters long, possibly produced during terrestrial freeze-thaw cycles, along which secondary iron oxides and hydroxides, and fine-grained whitish materials (possibly calcite and/or other carbonates) have developed. The interiors of most large specimens show minimal secondary iron oxide staining (weathering grade W1 of Wlotzka, 1993); smaller pieces show moderate (20–30%) oxidation of metal, suggesting grade W2. Partially preserved remnants of fusion crust <0.5 mm thick were observed on six small specimens; a few other pieces have smooth surfaces that may represent weathered fusion crust. Desert varnish, as is present in some other Namibian meteorites such as Gobabeb (Fudali and Noonan, 1975), is absent from all specimens of Korra Korrabes, consistent with the location of the recovery site ~100 km east of the major Namibian dune fields, and possibly indicating a relatively recent exposure of the specimens at the present deflation surface.

Cut surfaces of several pieces of Korra Korrabes reveal the presence of ~10–20% angular to irregular clasts that vary in size up to 3 cm across (Fig. 2). Most clasts have a lighter grey-brown colour with respect to the surrounding host material, resembling the so-called light-dark breccias that are common amongst ordinary chondrites (*e.g.*, Fredriksson and Keil, 1963; Bunch and Rajan, 1988; Wasson, 1974; Dodd, 1981). The bulk of the specimens, however, are composed of relatively uniform, dark grey-brown material in which abundant circular chondrules and irregular grains of Fe-Ni metals and sulfides are readily visible in a very fine-grained, dark brown matrix (Fig. 2). Discernible chondrules vary in size from <0.5–2 mm in diameter, and from whitish to dark grey in colour. Circular chondrules are present in some clasts, but in far lesser apparent


FIG. 2. Cut surface of Korra Korrabes, showing general textural features. A clast ~2 cm across is apparent at upper left. The darker grey-brown host material contains abundant round chondrules up to 2 mm in diameter.

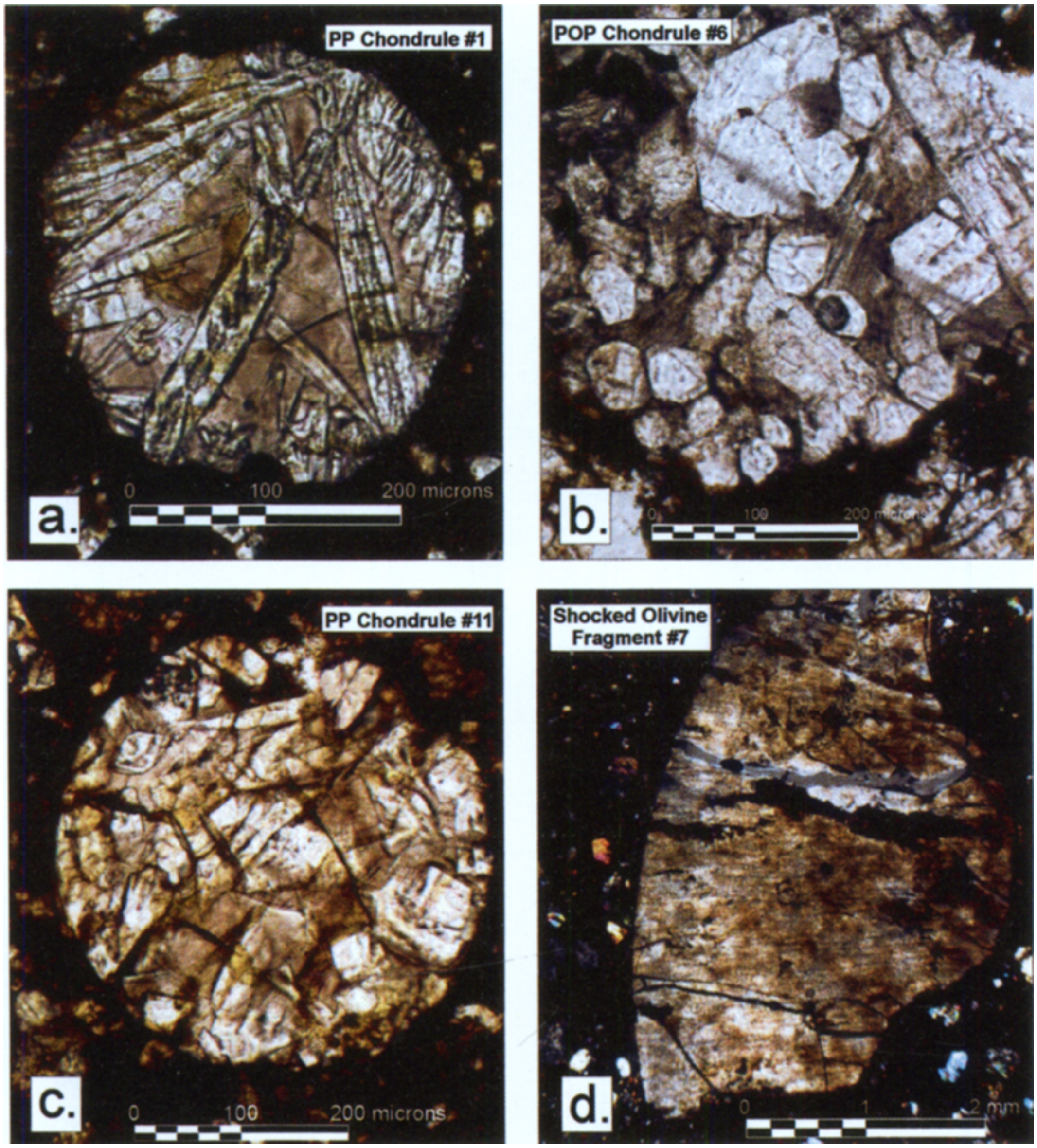


FIG. 3. Photomicrographs of chondrules and chondrule fragments in Korra Korrabes. (a) Pyroxene porphyritic chondrule #1 consists of elongate crystals of zoned clinoenstatite ($Fs_{0.2-20.9}$) surrounded by pink, Ca-free feldspathic glass. Plane polarized light. (b) Pyroxene-olivine porphyritic chondrule #6 contains euhedral, zoned olivine ($Fa_{14}$ to $Fa_{19}$) crystals and elongate, multiply-twinned low-Ca pyroxene (not analysed), surrounded by partially devitrified glass. Plane polarized light. (c) Pyroxene porphyritic chondrule #11, consisting of extremely high-Al (14–17.8 wt% $Al_2O_3$) Ca-rich pyroxene crystals, surrounded by pinkish, low-Ca feldspathic glass. Plane polarized light. (d) Olivine crystal ($Fa_{21-27}$) exhibiting mosaic structure indicative of shock. The curved edge suggests that this may be a fragment of a larger chondrule. Crossed polarizers.

abundance than within the surrounding host material. Metals are inhomogeneously distributed; most consist of small (<0.1–0.2 mm) grains, although larger (up to 10 mm), irregular to elongate grains of both metal and sulfide can be observed.

### Petrographic Observations

Examination of polished thin sections reveals that the bulk of Korra Korrabes material (excluding clasts) consists of round to irregular chondrules, chondrule and mineral fragments, and irregular Fe-Ni metal and sulfide grains, in an extremely fine-grained, variably oxidized, nearly opaque, clastic matrix. Recognized chondrule types, in order of decreasing abundance, include porphyritic olivine-pyroxene (POP; ~40%), porphyritic olivine (PO; ~28%), porphyritic pyroxene (PP; ~12%), barred olivine (BO; ~9%), excentroradial pyroxene (RP; ~7%), and granular pyroxene (GP; ~4%). The relative abundances of chondrule types are estimates based on observations of ~160 chondrules in several thin sections; the results are similar to those given by Gooding and Keil (1981). Measured chondrule diameters vary from 0.2 to 1.2 mm (mean = 0.56 ± 0.29 mm). Porphyritic chondrules (PO, POP and PP) generally contain euhedral to subhedral olivine and/or pyroxene phenocrysts, surrounded by glass (*e.g.*, chondrules #1, 6, 11, Fig. 3a,b,d), or less commonly, by cryptocrystalline mesostasis. Phenocryst shapes and sizes vary widely within and between chondrules, as does the crystal/glass ratio. Most pyroxenes are low-Ca clinobronzites, with well-developed multiple lamellar twinning and inclined extinction. A small proportion of POP chondrules contain low-Ca pyroxene phenocrysts that poikilitically surround irregular to rounded olivine inclusions or chadacrysts. Two atypical PP chondrules were found, one containing elongate, zoned clinoenstatite crystals (chondrule #1; Fig. 3a), and another with euhedral calcic clinopyroxene phenocrysts that have extremely high Al content (chondrule #11; Fig. 3d); in both cases, the pyroxene phenocrysts are surrounded by perfectly isotropic, pink glass. Glass in other porphyritic chondrules varies in colour from pink, to brownish, to opaque.

Barred olivine chondrules typically consist of parallel, optically continuous olivine platelets connected to a concentric outer olivine shell (*e.g.*, chondrule #2), although most of the varieties of BO chondrules described by Weisberg (1987) are also present in Korra Korrabes. Excentroradial pyroxene (RP) chondrules include those in which the pyroxene fibres radiate from a single point at the chondrule edge (*e.g.*, chondrule #9), or from several such points, resulting in mutually intersecting fan-like arrays. Rare granular pyroxene chondrules (*e.g.*, GP chondrule #3) consist of irregular aggregates of interlocking, multiply twinned, low-Ca pyroxene. All olivines in Korra Korrabes chondrules exhibit sharp optical extinction, with irregular fractures, and appear to be unshocked (shock stage S1 of Stöffler *et al.*, 1991).

The inter-chondrule matrix of Korra Korrabes consists of both types of materials described and defined by Scott *et al.* (1988) and Brearley and Jones (1998): heterogeneous clastic material consisting of mineral fragments of extremely variable size (1–200 $\mu$m) in a very fine-grained, nearly opaque matrix, and volumetrically lesser ultrafine, nearly opaque rims (width up to ~200 $\mu$m) around some chondrules and chondrule fragments. In both cases the fine-grained material contains substantial Fe-oxide staining. The vast majority of mineral fragments are irregular, unshocked olivines, generally in the size range 20–100 $\mu$m, that occur within the extremely fine-grained matrix or in the heterogeneous inter-chondrule regions. One example was found of a large (3.5 × 2 mm) olivine fragment (Fig. 3c), whose curved boundary suggests that it may represent a broken piece of a once larger chondrule with radius = 3–4 mm. Although obviously part of a single olivine crystal, this fragment exhibits two sets of nearly orthogonal planar fractures, and undulatory to coarse mosaic extinction pattern. These features are characteristic of moderate degrees of impact-related shock deformation (shock stage S3 of Stöffler *et al.*, 1991). Irregular grains of Fe-Ni metal, typically 100–1000 $\mu$m across, occur scattered throughout the matrix and inter-chondrule regions, although both larger (up to ~1 cm) and smaller grains are also present. The larger metal grains exhibit a peculiar spongiform texture, consisting of an interconnected network of irregular grains. Discrete grains of troilite have similar textural features to metals, but tend to be smaller, and are present in far lower abundance.

Because of their variable size and distribution (Fig. 2), clastic material is not present in all thin sections studied, although in a few cases, obvious clasts up to 1 cm across were discernable. Boundaries between clasts and surrounding host vary from sharply defined interfaces, to diffuse transitions, and at least some of the components constituting the matrix of Korra Korrabes represent variably comminuted clast materials. In cases where sharply defined clasts can be clearly discerned, their internal textures are invariably more heterogeneous and recrystallized with respect to the well-preserved magmatic textures present in the vast majority of Korra Korrabes chondrules. Most clasts consist of irregular aggregates of olivine, low-Ca pyroxene and Fe-Ni metal, although euhedral to subhedral crystals of both mafic silicates up to several hundred microns across have been observed. Olivines dominantly show sharp extinction, although in some clasts slight undulatory extinction suggests shock stage S2 of Stöffler *et al.* (1991). Both twinned and untwinned low-Ca pyroxenes are present, suggesting variable preservation of monoclinic structure. Some of the larger clasts themselves contain internal clast fragments, whose textures range from granoblastic to cryptocrystalline.

## Mineral Compositions

**Olivines**–A total of 152 microprobe analyses were obtained for olivine in five chondrules, as well as for crystal fragments in the inter-chondrule matrix; compositions are plotted in Fig. 4, and representative analyses are given in Table 2. The compositional spread for all analysed olivine in Korra Korrabes is $Fa_{13.8}$–$Fa_{27.2}$ (mean = $Fa_{18.59\pm2.25}$; all reported standard deviations are 1$\sigma$), with percent mean deviation (Dodd *et al.*, 1967) = 7.82%. CaO content varies from 0–0.20 wt% (mean = 0.05 ± 0.05 wt% CaO); there is no clear-cut relationship between Fa and CaO content, as has been reported for olivines in many chondrite types (*e.g.*, Scott and Taylor, 1983).

Olivine compositions show variable degrees of heterogeneity within and between individual chondrules. The most homogeneous compositions are found in barred olivine chondrules (*e.g.*, BO chondrule #2; $Fa_{18.78}$–$Fa_{20.35}$). Some porphyritic chondrules contain large, normally zoned, euhedral olivine phenocrysts with up to 5 mol% compositional variation (*e.g.*, POP chondrule #6, core = $Fa_{13.8}$, rim = $Fa_{18.9}$; Fig. 3b). Smaller euhedral olivine phenocrysts in other chondrules (*e.g.*, POP chondrule #8) are either unzoned, or very weakly zoned. The large olivine fragment that shows evidence for shock-induced mosaicism (chondrule fragment #7; Fig. 3c) exhibits fairly large compositional variation of over 6 mol%, from $Fa_{20.69}$ to $Fa_{26.93}$ (Fig. 4). Random microprobe analyses of small olivine fragments in the matrix of Korra Korrabes show a large compositional spread from $Fa_{18.21}$ to $Fa_{27.17}$ (Fig. 4).

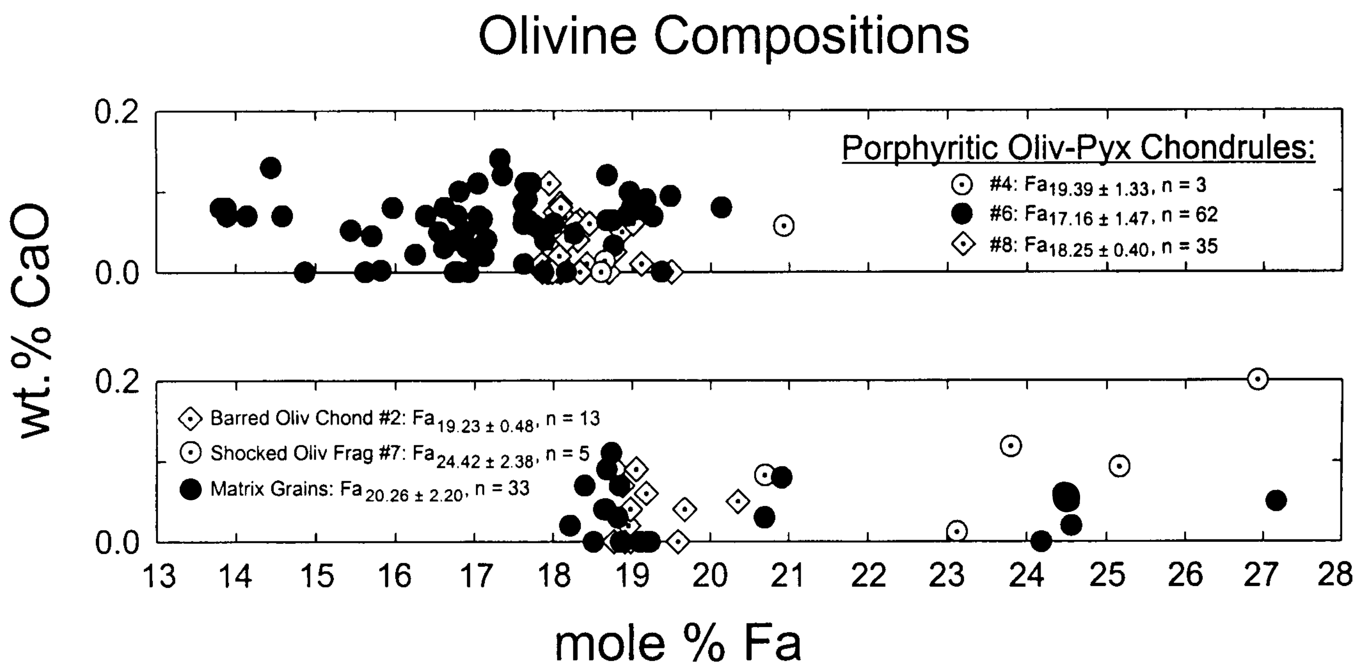


FIG. 4. Olivine compositions for individual chondrules and mineral fragments, plotted on diagrams of mol% Fa *vs.* wt% CaO.

TABLE 2. Representative microprobe analyses of olivines from the Korra Korrabes chondrite.

| Chondrule Type | #2 BO | #4 POP | #6 POP | #7 CH FRAG | #8 POP | MATRIX FRAG |
|---|---|---|---|---|---|---|
| $SiO_2$ | 39.50 | 40.34 | 39.78 | 39.49 | 40.23 | 39.02 |
| $TiO_2$ | 0.04 | 0.06 | 0.03 | 0.04 | 0.08 | 0.00 |
| FeO* | 18.44 | 17.57 | 15.90 | 19.39 | 16.89 | 22.50 |
| MnO | 0.27 | 0.42 | 0.54 | 0.48 | 0.40 | 0.19 |
| MgO | 42.18 | 43.11 | 43.76 | 41.70 | 42.89 | 39.01 |
| CaO | 0.04 | 0.00 | 0.00 | 0.08 | 0.09 | 0.06 |
| Total | 100.47 | 101.50 | 100.01 | 101.19 | 100.57 | 100.78 |
| **Cations per 4 oxygens** | | | | | | |
| Si | 1.002 | 1.008 | 1.003 | 1.000 | 1.012 | 1.005 |
| Ti | 0.001 | 0.001 | 0.001 | 0.001 | 0.001 | 0.000 |
| Fe | 0.391 | 0.367 | 0.335 | 0.411 | 0.355 | 0.485 |
| Mn | 0.006 | 0.009 | 0.012 | 0.010 | 0.008 | 0.004 |
| Mg | 1.596 | 1.606 | 1.645 | 1.575 | 1.608 | 1.498 |
| Ca | 0.001 | 0.000 | 0.000 | 0.002 | 0.002 | 0.002 |
| Total | 2.997 | 2.991 | 2.996 | 2.999 | 2.986 | 2.994 |
| Fa | 19.69 | 18.61 | 16.93 | 20.69 | 18.10 | 24.45 |

*Total Fe as FeO.
Abbreviations: BO = barred olivine; POP = porphyritic olivine-pyroxene; CH FRAG = chondrule fragment; FRAG = fragment.

**Pyroxenes**–A total of 107 microprobe analyses of pyroxene were obtained for 8 individual chondrules. Compositions are plotted in a series of pyroxene quadrilateral diagrams in Fig. 5; representative analyses are given in Table 3. Most pyroxenes are low-Ca clinobronzites or clinoenstatites, whose compositions vary within and between chondrules from $Fs_{0.16}$ to $Fs_{27.80}$ and from $Wo_{0.36}$ to $Wo_{7.27}$ (mean = $Fs_{14.16\pm7.10}$; $Wo_{2.14\pm1.84}$, $n$ = 88). Excluding the unusually Mg- and Ca-rich clinoenstatites from PP chondrule #1 (Fig. 3a) reduces the compositional variability of low-Ca pyroxenes in Korra

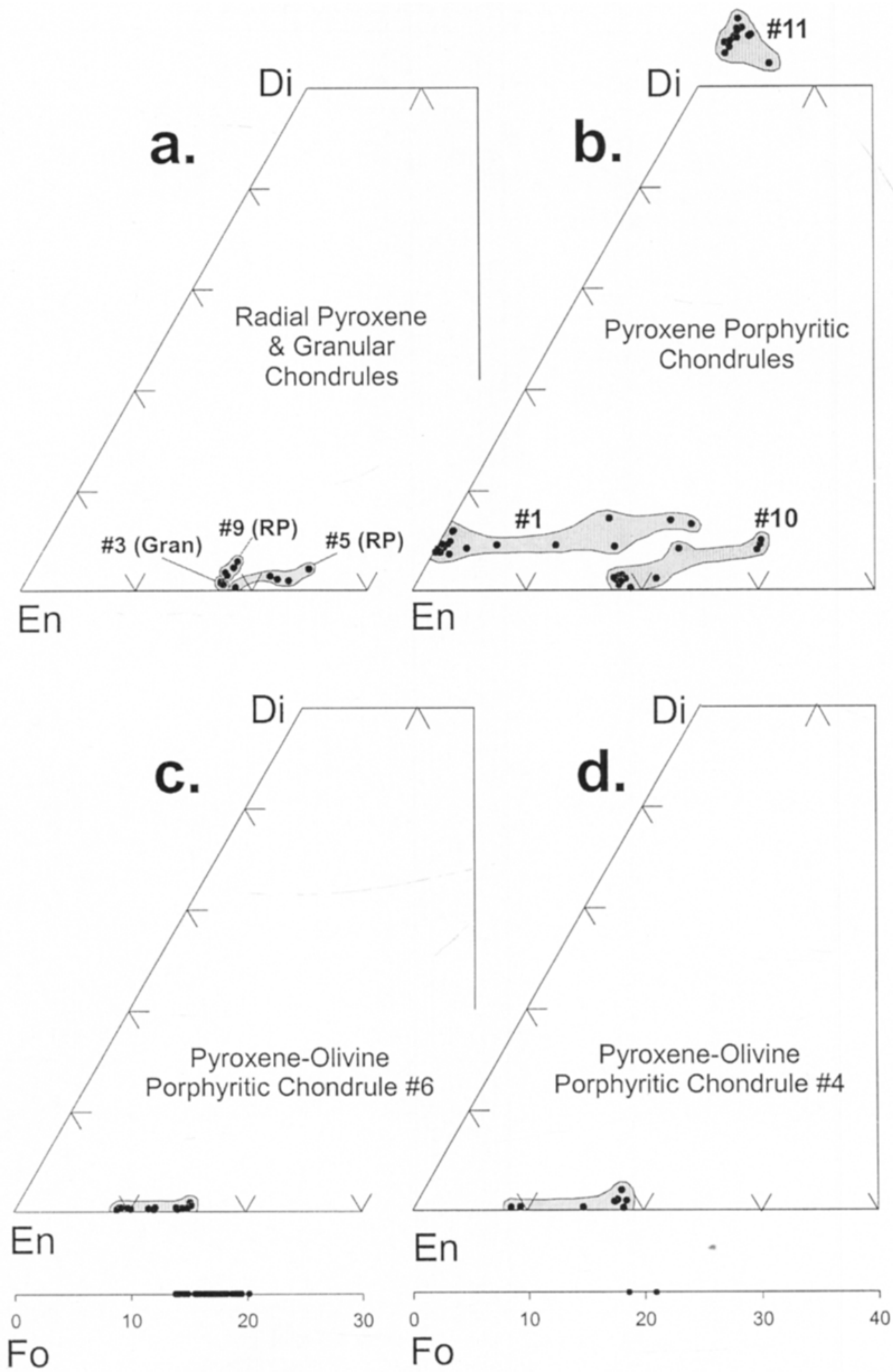


FIG. 5. Compositions of pyroxenes in Korra Korrabes chondrules. The high-Ca pyroxenes of PP chondrule #11 shown in (b) plot above the Di-Hd join because of major non-quadrilateral components. Coexisting olivine compositions for POP chondrules #6 and 4 are shown in (c) and (d).

TABLE 3. Representative microprobe analyses of pyroxenes from the Korra Korrabes chondrite.

| Chondrule | #1 | #3 | #4 | #5 | #6 | #9 | #10 | #11 |
|---|---|---|---|---|---|---|---|---|
| Type | PP | GP | POP | RP | POP | RP | PP | PP |
| $SiO_2$ | 57.80 | 56.31 | 58.35 | 54.72 | 57.51 | 55.97 | 56.62 | 45.04 |
| $TiO_2$ | 0.87 | 0.29 | 0.15 | 0.01 | 0.06 | 0.07 | 0.04 | 1.32 |
| $Al_2O_3$ | 2.63 | 0.00 | 0.00 | 0.00 | 0.00 | 0.84 | 0.00 | 16.45 |
| $Cr_2O_3$ | 0.22 | 0.12 | 0.46 | 0.41 | 0.58 | 0.58 | 0.00 | 0.44 |
| FeO* | 0.38 | 11.38 | 5.79 | 15.39 | 5.88 | 10.72 | 11.63 | 1.07 |
| MnO | 0.05 | 0.50 | 0.00 | 0.45 | 0.40 | 0.44 | 0.57 | 0.00 |
| MgO | 36.10 | 30.52 | 35.34 | 26.80 | 33.98 | 28.73 | 30.74 | 12.89 |
| NiO | 0.12 | 0.05 | 0.00 | 0.00 | 0.17 | 0.00 | 0.00 | 0.00 |
| ZnO | 0.36 | 0.00 | 0.06 | 0.59 | 0.18 | 0.00 | 0.00 | 0.00 |
| CaO | 2.03 | 0.38 | 0.24 | 1.13 | 0.26 | 0.78 | 0.58 | 23.01 |
| $Na_2O$ | 0.00 | 0.00 | 0.00 | 0.00 | 0.00 | 0.00 | 0.00 | 0.05 |
| $K_2O$ | 0.03 | 0.01 | 0.00 | 0.00 | 0.02 | 0.00 | 0.01 | 0.01 |
| Total | 100.59 | 99.56 | 100.39 | 99.50 | 99.04 | 98.13 | 100.19 | 100.28 |
| | | | | **Cations per 6 oxygens** | | | | |
| Si | 1.942 | 1.998 | 1.997 | 1.992 | 2.003 | 2.008 | 1.999 | 1.623 |
| $Al^{IV}$ | 0.058 | 0.000 | 0.000 | 0.000 | 0.000 | 0.000 | 0.000 | 0.377 |
| Total | 2.000 | 1.998 | 1.997 | 1.992 | 2.003 | 2.008 | 1.999 | 2.000 |
| $Al^{VI}$ | 0.046 | 0.000 | 0.000 | 0.000 | 0.000 | 0.036 | 0.000 | 0.322 |
| Ti | 0.022 | 0.008 | 0.004 | 0.000 | 0.002 | 0.002 | 0.001 | 0.036 |
| Cr | 0.006 | 0.003 | 0.012 | 0.012 | 0.016 | 0.016 | 0.000 | 0.013 |
| Fe | 0.011 | 0.338 | 0.166 | 0.469 | 0.171 | 0.322 | 0.343 | 0.032 |
| Mn | 0.001 | 0.015 | 0.000 | 0.014 | 0.012 | 0.013 | 0.017 | 0.000 |
| Mg | 1.808 | 1.614 | 1.803 | 1.455 | 1.764 | 1.537 | 1.618 | 0.692 |
| Ni | 0.003 | 0.001 | 0.000 | 0.000 | 0.005 | 0.000 | 0.000 | 0.000 |
| Zn | 0.009 | 0.000 | 0.002 | 0.016 | 0.005 | 0.000 | 0.000 | 0.000 |
| Ca | 0.073 | 0.014 | 0.009 | 0.044 | 0.010 | 0.030 | 0.022 | 0.888 |
| Na | 0.000 | 0.000 | 0.000 | 0.000 | 0.000 | 0.000 | 0.000 | 0.003 |
| K | 0.001 | 0.000 | 0.000 | 0.000 | 0.001 | 0.000 | 0.000 | 0.000 |
| Total | 1.981 | 1.993 | 1.993 | 2.001 | 1.988 | 1.956 | 2.001 | 1.986 |
| Wo | 3.86 | 0.74 | 0.45 | 2.24 | 0.50 | 1.59 | 1.11 | 55.07 |
| En | 95.57 | 82.09 | 91.17 | 73.94 | 90.70 | 81.37 | 81.58 | 42.93 |
| Fs | 0.56 | 17.17 | 8.38 | 23.82 | 8.80 | 17.04 | 17.31 | 2.00 |

*Total Fe as FeO
Abbreviations: POP = porphyritic olivine-pyroxene; PP = porphyritic pyroxene; GP = granular pyroxene; RP = excentroradial pyroxene.

Korrabes to $Fs_{8.37}$–$Fs_{27.80}$ and $Wo_{0.35}$–$Wo_{5.04}$ (mean = $Fs_{16.92\pm4.22}$ ; $Wo_{1.31\pm1.00}$, $n$ = 68).

As with olivines, compositions of pyroxenes vary in terms of Fe/(Fe + Mg), concentrations of minor element substituents, and degree of homogeneity, depending upon chondrule petrographic type. The most restricted compositions are found in granular pyroxene chondrule #3 ($Fs_{16.81}$–$Fs_{17.17}$), and to a lesser extent, in RP chondrules #9 ($Fs_{16.76}$–$Fs_{17.26}$) and #5 ($Fs_{18.33}$–$Fs_{23.81}$) (Fig. 5a). Some of the compositional variability of pyroxenes in RP chondrule #9 may be caused by variable incorporation of very fine-grained feldspathic glass, as indicated by positive correlations of $Na_2O$ and $Al_2O_3$. No such correlations are apparent for RP chondrule #5, suggesting that the observed 5.5 mol% range in Fs is likely to reflect actual variability in pyroxene composition (Fig. 5a).

Pyroxene phenocrysts in porphyritic chondrules (PP or POP) display distinct compositional zoning, with enrichments in Fs and Wo components toward crystal edges. This is most prominently exhibited in the elongate clinoenstatite crystals of PP chondrule #1 (Fig. 3a), which show normal zoning of nearly 21 mol%, from cores of $Fs_{0.16}Wo_{3.69}$ to rims of $Fs_{20.91}Wo_{7.27}$ (Fig. 5b). This chondrule appears to be atypical of Korra Korrabes chondrules, in that its pyroxenes are unusually Mg-, Ca- and Al-rich (1.28–3.87 wt% $Al_2O_3$), and are surrounded by pink glass with peculiar Ca-free composition, as discussed below.

TABLE 4. Mean compositions of glasses in the Korra Korrabes chondrite.*

| Chondrule Type | #1 PP Pink glass ($n$ = 10) | #2 BO ($n$ = 2) | #6 POP ($n$ = 3) | #11 PP Pink glass ($n$ = 18) | #7 Shocked Ol Fragment ($n$ = 1) |
|---|---|---|---|---|---|
| $SiO_2$ | 58.04 ± 1.45 | 58.41 ± 0.22 | 65.98 ± 0.80 | 55.95 ± 1.12 | 65.38 |
| $TiO_2$ | 0.71 ± 0.23 | 0.71 ± 0.23 | 0.51 ± 0.11 | 0.99 ± 0.30 | 0.54 |
| $Al_2O_3$ | 23.29 ± 0.81 | 20.34 ± 0.14 | 14.68 ± 0.93 | 25.79 ± 0.83 | 16.96 |
| $Cr_2O_3$ | 0.19 ± 0.16 | 0.48 ± 0.06 | 0.05 ± 0.05 | 0.05 ± 0.06 | 0.11 |
| MgO | 0.32 ± 0.25 | 2.81 ± 0.21 | 2.43 ± 1.00 | 0.49 ± 0.84 | 2.51 |
| FeO† | 1.32 ± 0.38 | 1.99 ± 0.13 | 3.01 ± 0.58 | 1.34 ± 0.67 | 2.36 |
| MnO | 0.13 ± 0.11 | 0.11 ± 0.02 | 0.09 ± 0.08 | 0.06 ± 0.07 | 0.03 |
| NiO | 0.05 ± 0.11 | 0.09 ± 0.13 | 0.76 ± 0.46 | 0.13 ± 0.15 | 0.25 |
| ZnO | 0.33 ± 0.37 | 0.20 ± 0.20 | 0.11 ± 0.13 | 0.10 ± 0.15 | 0.04 |
| $ZrO_2$ | 0.01 ± 0.04 | 0.00 ± 0.00 | 0.00 ± 0.00 | 0.01 ± 0.06 | 0.13 |
| CaO | 0.00 ± 0.00 | 3.02 ± 0.19 | 2.03 ± 1.88 | 0.75 ± 0.96 | 4.54 |
| $Na_2O$ | 9.31 ± 1.25 | 12.70 ± 1.09 | 9.51 ± 0.54 | 12.93 ± 0.82 | 9.10 |
| $K_2O$ | 6.98 ± 0.16 | 0.19 ± 0.06 | 0.12 ± 0.20 | 0.67 ± 0.10 | 0.28 |
| Cl | 0.08 ± 0.04 | 0.05 ± 0.07 | 0.07 ± 0.00 | 0.01 ± 0.02 | 0.00 |
| Total | 100.76 | 101.07 | 99.35 | 99.27 | 102.23 |
| | | | **CIPW Norms** | | |
| Q | – | – | 2.25 | – | 0.03 |
| Cor | 0.42 | – | – | 2.43 | – |
| Or | 41.25 | 1.12 | 0.71 | 3.96 | 1.66 |
| Ab | 27.74 | 54.19 | 77.48 | 56.93 | 77.00 |
| An | – | – | – | 3.72 | 4.60 |
| Ne | 27.64 | 27.74 | – | 28.43 | – |
| Cpx | – | 13.67 | 10.81 | – | 14.60 |
| Opx | – | 2.06 | 6.85 | – | 2.98 |
| Oliv | 1.65 | 1.35 | – | 1.72 | – |
| Ilm | 1.35 | 0.71 | 0.97 | 1.88 | 1.03 |
| Chr | 0.28 | – | 0.02 | 0.07 | 0.16 |
| Total | 100.33 | 100.84 | 99.09 | 99.14 | 102.06 |

*Standard deviations are 1$\sigma$.
†Total Fe as FeO.
Abbreviations: PP = porphyritic pyroxene; BO = barred olivine; POP = porphyritic olivine-pyroxene; Ol = olivine.

More typically, low-Ca pyroxenes in PP or PO chondrules (*e.g.*, # 4,6 and 10) are higher in Fs and lower in Wo components ($Fs_{8.72-27.80}$, $Wo_{0.36-5.05}$), although both Fs and Wo components also increase from cores to rims (Fig. 5b–d). Low-Ca pyroxene phenocrysts have lower Wo contents in olivine-bearing (POP) chondrules relative to olivine-free (PP) types (Fig. 5b–d).

Another unusual chondrule (PP #11; Fig. 3d) was found that consists solely of high-Ca pyroxene phenocrysts surrounded by Ca-depleted feldspathic glass (described below). These pyroxenes are extremely aluminous (14.0–17.82 wt% $Al_2O_3$), and are also enriched in other non-quadrilateral components such as Ti (0.91–2.11 wt% $TiO_2$); accordingly, their compositions cluster in a field above the pyroxene quadrilateral (Fig. 5b). Mineral formulae (Table 3) yield 18.5–25.4 mol% non-quadrilateral components, dominantly Ca-Tschermak's molecule.

**Glasses**–Microprobe analyses of glasses were obtained for five petrographically distinct chondrule types (Table 4). Because a defocused electron beam was needed to minimize alkali volatilisation, it was difficult to avoid variable incorporation of olivine or pyroxene crystals in the analyses for those chondrules in which glass occurs in small intracrystalline regions (*e.g.*, chondrules #2, #6, and #7; Fig. 3b,c). In such cases, the oxide components of the analyses plot as linear arrays that project toward the compositions of associated crystals; glass compositions can be approximated by selecting those analyses farthest from crystal compositions. For example, two analyses (selected as most representative of crystal-free compositions from 11 analyses) of glass occurring between optically continuous olivine plates in barred olivine chondrule #2 are rich in $Na_2O$, $Al_2O_3$ and $SiO_2$, with notable but minor CaO, MgO and FeO

TABLE 5. Mean compositions of kamacite and troilite in the Korra Korrabes chondrite.

| | Mean kamacite* ($n$ = 17) | Mean troilite* | |
|---|---|---|---|
| Fe | 93.21 ± 0.80 | 64.05 ± 0.59 | ($n$ = 19) |
| Cu | 0.04 ± 0.06 | 0.05 ± 0.08 | ($n$ = 19) |
| Ni | 6.51 ± 0.53 | 0.11 | ($n$ = 1) |
| Zn | n.a. | 0.30 | ($n$ = 1) |
| Te | n.a. | 0.03 | ($n$ = 1) |
| Sb | n.a. | 0.13 | ($n$ = 1) |
| Co | 0.64 ± 0.19 | 0.14 ± 0.15 | ($n$ = 19) |
| Mn | n.a. | 0.08 | ($n$ = 1) |
| S | 0.01 ± 0.01 | 35.75 ± 0.86 | ($n$ = 19) |
| As | n.a. | 0.15 | ($n$ = 1) |
| | 100.41 | 100.79 | |

*Standard deviations are 1$\sigma$.
n.a. = not analysed.

(Table 4). These glasses are highly enriched in albite components, but are overly deficient in silica to represent true feldspar compositions. Their strongly nepheline-normative character is illustrated by the CIPW norms given in Table 4.

For pyroxene-olivine porphyritic chondrule #6, three glass compositions (selected from nine defocused-beam analyses) are higher in $SiO_2$ and lower in alkalies and alumina than those in the barred olivine chondrule (Table 4), and are closer to stoichiometric feldspar compositions of approximately $Ab_{78-97}Or_{0-2}$. A single glass composition from shocked olivine chondrule fragment #7 (selected from eight analyses; Table 4) is similar, and also approximates albite-rich feldspar (~$Ab_{77}Or_2$).

In other chondrules (*e.g.*, #1, 11; Fig. 3a,d), glass is sufficiently abundant such that crystals can be avoided in defocused-beam analyses, and measured compositional variations may represent actual chemical diversity in glasses. In pyroxene porphyritic chondrule #11 (Fig. 3d), interstitial glass between high-Ca and -Al clinopyroxene phenocrysts is extremely enriched in $Na_2O$ (11.5–14.7 wt%) and $Al_2O_3$ (24.2–27.3 wt%), but depleted in CaO (0.13–3.63 wt%, avg. = 0.75 ± 0.96 wt%, $n$ = 18). Such compositions are unusual for glasses in typical chondrites. The pink glass observed in pyroxene porphyritic chondrule #1 (Fig. 3a) is also compositionally unusual, and appears to be CaO-free, with high $K_2O$ (6.1–7.2 wt%), $Na_2O$ (8.0–10.4 wt%) and $Al_2O_3$ (21.9–24.2 wt%). Also surprising are the high ZnO (to 1.1 wt%) and Cl (to 0.11 wt%) contents in some of the analysed glasses (Table 4).

**Metals and Sulfides**–Compositions of metallic Fe-Ni were determined for several large (100–500 $\mu$m), irregular grains associated with matrix material between chondrules. Results for kamacite ($n$ = 17; Table 5) show modest variations in Fe (91.9–94.6 wt%, avg. = 93.21 ± 0.78 wt%), Ni (4.8–7.2 wt%, avg. = 6.51 ± 0.51 wt%) and Co (0.11–0.94 wt%, avg. = 0.64 ± 0.19 wt%). Taenites were not encountered during reconnaissance microprobe work. Troilite compositions ($n$ = 19; Table 5) also show modest variations in Fe (63.2–65.2 wt%, avg.= 64.05 ± 0.59 wt%) and S (32.9–36.5 wt%, avg.= 35.75 ± 0.86 wt%). One more extensive spot analysis of troilite yields Ni = 0.11 wt%, Zn = 0.30 wt%, Sb = 0.13 wt% and Te = 0.03 wt%; concentrations of Se, Bi, Cd, Ag and Au were below detection limits of our microprobe instrument.

## DISCUSSION

### Classification

The classification of chondritic breccias is usually based upon the mineralogy and textures of the host material, rather than that of clasts, which are commonly more equilibrated than their host (Van Schmus and Wood, 1967; Dodd, 1974). The following features of the dominant host material suggest that Korra Korrabes should properly be classified as an H3 chondrite. The mean Fe/(Fe + Mg) of analysed olivine and low-Ca pyroxene (excluding the Mg-rich clinoenstatites of PP chondrule #1) plots within the field for H-group equilibrated chondrites. Other results consistent with classification of Korra Korrabes in the H chemical group include the Co content of kamacite (mean = 0.64 ± 0.19 wt%; Table 5), which corresponds to those of other H chondrites (<0.9 wt% Co; Sears and Weeks, 1986; Rubin, 1990).

Classification of Korra Korrabes as petrologic type 3 is indicated by the near-pristine igneous textures and excellent preservation of glass within many chondrules (Fig. 3), the compositional variability and presence of magmatic zoning in olivine and pyroxene phenocrysts (Figs. 3–5), the dominance of twinned clinobronzite and clinoenstatite in the pyroxene assemblage, and the apparent absence of chromite, taenite and crystalline plagioclase. Other features indicative of a type 3 classification include the Ni content of troilite (0.11 wt%, albeit from one analysis; Table 5) (Wood, 1967). Characterization of the metamorphic subtype (Sears *et al.*, 1980) awaits thermoluminescence studies, which are in progress.

Although a detailed study of clast materials in Korra Korrabes has not yet been carried out, all clasts observed thus far exhibit recrystallized textures, and therefore are of higher petrologic type (5–6) than their host. Some clasts show evidence for a slightly higher level of shock metamorphism (stage S2) relative to the bulk of the host, which is unshocked; at least one chondrule fragment shows moderate shock (stage S3). Based on estimated metal abundances, most clasts appear to be H-chondrites, but proper classification awaits detailed petrographic and microprobe studies.

### Noteworthy Features

The abundant presence of well-preserved glass in many Korra Korrabes chondrules and in some cases, their unusual composition, is worthy of further discussion. Of particular interest are the pink glasses in PP chondrules #1 and 11 (Fig. 3a,d; Table 4). The glass in chondrule #1 is Ca-free and highly alkaline (mean $Na_2O + K_2O$ = 16.3 wt%; Table 4), and seemingly out of equilibrium with the elongate, normally zoned, Mg-rich and Ca-bearing clinoenstatites that resemble quench crystals (Fig. 3a). Likewise, the Ca-deficient (mean CaO = 0.75 wt%; Table 4), Na-rich (mean $Na_2O$ = 12.9 wt%) glass in chondrule #11 seems unlikely to represent a liquid capable of crystallizing the remarkably aluminous calcic clinopyroxenes it contains (Fig. 3d). Ca-deficient glasses (CaO = 0.14–0.89 wt%), in some cases pink in colour, have been reported in Krahenberg (LL5), Parnallee (LL3.6) and Yamato-74191 (L3) (McCoy *et al.*, 1991; Kimura and Yagi, 1980), although their compositions are not as alkaline as those observed in Korra Korrabes. As a large (~140 kg), brecciated ordinary chondrite of low metamorphic grade (H3), Korra Korrabes represents an ideal target for further study of these apparent magmatic disequilibrium features, and chondrule- and chondrite-forming processes in general.

*Acknowledgements*–Bruce Cairncross put me in contact with Ronnie McKenzie, who generously provided Korra Korrabes material for characterization and study, as well as information on its recovery. Microprobe analyses were done by Belinda Van Lente, with the assistance of Nellie Day. Kimmie Hisada provided nice digital photos of the cut specimens, and Mike Knoper and Jan-Marten Huizenga helped with the digital photomicrography. Discussions with Jeff Grossman, Mike Zolensky and Roger Hewins on chondrite petrology, petrography and classification helped enormously. Substantial improvements to this paper resulted from reviews by Phil Bland and Rosa Scorzelli, and Dave Mittlefehldt supplied sound editorial advice. This study was supported by the South African National Research Foundation and Dr. R. McKenzie.

*Editorial handling:* D. W. Mittlefehldt

## REFERENCES

BREARLEY A. J. AND JONES R. H. (1998) Chondritic meteorites. In *Planetary Materials* (ed. J. J. Papike), pp. 3-1 to 3-398. Rev. Mineral **36**, Mineral. Soc. Amer., Washington, D.C., USA.

BUCHWALD V. F. (1969a) "Bushman Land" and "Karasburg", two new iron meteorites from SW Africa (abstract). *Meteoritics* **4**, 265–266.

BUCHWALD V. F. (1969b) The Gibeon meteorites (abstract). *Meteoritics* **4**, 264–265.

BUCHWALD V. F. (1975) *Handbook of Iron Meteorites*. Univ. California Press, Berkeley, California, USA. 1418 pp.

BUNCH T. E. AND RAJAN R. S. (1988) Meteorite regolith breccias. In *Meteorites and the Early Solar System* (ed. J. F. Kerridge), pp. 144–164. Univ. Arizona Press, Tucson, Arizona, USA.

CLARKE R. S., JR. (1975) The Meteoritical Bulletin No. 53, 1975: Fall of the Ovambo, South West Africa, stony meteorite. *Meteoritics* **10**, 137–138.

DODD R. T. (1974) Petrology of the St. Mesmin chondrite. *Contrib. Mineral. Petrol.* **46**, 129–145.

DODD R. T. (1981) *Meteorites*. Cambridge Univ. Press, Cambridge, U.K. 368 pp.

DODD R. T., VAN SCHMUS W. R. AND KOFFMAN D. M. (1967) A survey of the unequilibrated ordinary chondrites. *Geochim. Cosmochim. Acta* **31**, 921–951.

FREDRIKSSON K. AND KEIL K. (1963) The light-dark structure in the Pantar and Kapoeta stone meteorites. *Geochim. Cosmochim. Acta* **27**, 717–739.

FRICK C. AND HAMMERBECK E. C. I. (1973) Catalogue of South African and South West African meteorites (abstract). *Geol. Survey S. Afr. Bull.* **57**, 47.

FUDALI R. F. AND NOONAN F. (1975) Gobabeb, a new chondrite: The coexistence of equilibrated silicates and unequilibrated spinels. *Meteoritics* **10**, 31–39.

GOODING J. L. AND KEIL K. (1981) Relative abundances of chondrule primary textural types in ordinary chondrites and their bearing on conditions of chondrule formation. *Meteoritics* **16**, 17–43.

GRAHAM A. L. (1978) Meteoritical Bulletin No. 55, 1978 September: Discovery of the St. Francis Bay, South West Africa, stony meteorite. *Meteoritics* **13**, 348.

GRAHAM A. L. (1981) Meteoritical Bulletin No. 59, 1981 June: Discovery of the Namib Desert, Namibia, stony meteorite. *Meteoritics* **16**, 196.

HUSS G. I. (1982) Sorting out the many falls of the Tulia-Dimmitt area (abstract). *Meteoritics* **17**, 229–230.

KIMURA M. AND YAGI K. (1980) Crystallization of chondrules in ordinary chondrites. *Geochim. Cosmochim. Acta* **44**, 589–602.

MCCOY T. J., SCOTT E. R. D., JONES R. H., KEIL K. AND TAYLOR G. J. (1991) Composition of chondrule silicates in LL3-5 chondrites and implications for the nebular history and parent body metamorphism. *Geochim. Cosmochim. Acta* **55**, 601–619.

REID A. M., JAKES P., ZOLENSKY M. E. AND MILLER R. MCG. (1995) Recovery of three ordinary chondrites, Rooikop 001–003, from the Namib Desert in Western Namibia. *Meteoritics* **30**, 781–784.

RUBIN A. E. (1990) Kamacite and olivine in ordinary chondrites: Intergroup and intragroup variations. *Geochim. Cosmochim. Acta* **54**, 1217–1232.

RUSSELL S. S., ZOLENSKY M. E., BLAND P. A., GENGE M. J., GRADY M. M. AND HUTCHINSON R. (1999) The distribution of meteorite finds in the Namibian desert and recovery of a highly shocked meteorite pairing group (abstract). *Lunar Planet. Sci.* **31**, #1743, Lunar and Planetary Institute, Houston, Texas, USA (CD-ROM).

SCOTT E. R. D. AND TAYLOR G. J. (1983) Chondrules and other components in C, O and E chondrites: Similarities in their properties and origin. *J. Geophys. Res.* **88**, B275–B286.

SCOTT E. R. D. AND WASSON J. T. (1976) Chemical classification of iron meteorites: VIII, Groups IC, IIE, IIIF and 97 other irons. *Geochim. Cosmochim. Acta* **40**, 103–115.

SCOTT E. R. D., BARBER D. J., ALEXANDER C. M., HUTCHINSON R. AND PECK J. A. (1988) Primitive material surviving in chondrites: Matrix. In *Meteorites and the Early Solar System* (ed. J. F. Kerridge), pp. 718–745. Univ. Arizona Press, Tucson, Arizona, USA.

SEARS D. W. G. AND WEEKS K. S. (1986) Chemical and physical studies of type 3 chondrites. VI: Siderophile elements in ordinary chondrites. *Geochim. Cosmochim. Acta* **50**, 2815–2832.

SEARS D. W. G., GROSSMAN J. N., MELCHER C. L., ROSS L. M. AND MILLS A. A. (1980) Measuring metamorphic history of unequilibrated ordinary chondrites. *Nature* **287**, 791–795.

SPENCER L. J. AND HEY M. H. (1932) Hoba (South West Africa), the largest known meteorite. *Mineral. Mag.* **23**, 1–18.

STÖFFLER D., KEIL K. AND SCOTT E. R. D. (1991) Shock metamorphism of ordinary chondrites. Effects in meteorites. *Geochim. Cosmochim. Acta* **55**, 3845–3867.

VAN SCHMUS W. AND WOOD J. (1967) A chemical-petrologic classification for the chondritic meteorites. *Geochim. Cosmochim. Acta* **31**, 747–765.

WASSON J. T. (1974) *Meteorites. Minerals and Rocks.* Springer-Verlag, New York, New York, USA. 316 pp.

WEISBERG M. K. (1987) Barred olivine chondrules in ordinary chondrites. *Proc. Lunar Planet. Sci. Conf.* **17th**, *J. Geophys. Res.* **92**, E663–E678.

WLOTZKA F. (1991) The Meteoritical Bulletin No. 71, 1991 September. *Meteoritics* **26**, 255–262.

WLOTZKA F. (1993) A weathering scale for ordinary chondrites (abstract). *Meteorit. Planet. Sci.* **28**, 460.

WOOD J. A. (1967) Chondrites: Their metallic minerals, thermal histories, and parent bodies. *Icarus* **3**, 429–459.